Demonstration of Einstein-Podolsky-Rosen Steering Using Single-Photon Path Entanglement and Displacement-Based Detection

T. Guerreiro,[1] F. Monteiro,[1] A. Martin,[1] J. B. Brask,[2] T. Vértesi,[3] B. Korzh,[1] M. Caloz,[1] F. Bussières,[1] V. B. Verma,[4] A. E. Lita,[4] R. P. Mirin,[4] S. W. Nam,[4] F. Marsilli,[5] M. D. Shaw,[5] N. Gisin,[1] N. Brunner,[2,*] H. Zbinden,[1] and R. T. Thew[1,†]

[1]*Group of Applied Physics, University of Geneva, CH-1211 Geneva 4, Switzerland*

[2]*Département de Physique Théorique, Université de Genève, CH-1211 Geneva 4, Switzerland*

[3]*Institute for Nuclear Research, Hungarian Academy of Sciences, H4001-Debrecen, P.O. Box 51, Hungary*

[4]*National Institute of Standards and Technology, 325 Broadway, Boulder, Colorado 80305, USA*

[5]*Jet Propulsion Laboratory, California Institute of Technology, 4800 Oak Grove Drive, Pasadena, California 91109, USA*

(Received 11 March 2016; published 12 August 2016)

We demonstrate the violation of an Einstein-Podolsky-Rosen steering inequality developed for single-photon path entanglement with displacement-based detection. We use a high-rate source of heralded single-photon path-entangled states, combined with high-efficiency superconducting-based detectors, in a scheme that is free of any postselection and thus immune to the detection loophole. This result conclusively demonstrates single-photon entanglement in a one-sided device-independent scenario, and opens the way towards implementations of device-independent quantum technologies within the paradigm of path entanglement.

DOI: 10.1103/PhysRevLett.117.070404

Single-photon entanglement is not only one of the simplest forms of entanglement to generate, it is both fundamentally fascinating and potentially practical. At times its mere existence was debated [1,2]; however, today it lies at the heart of key quantum information protocols, such as quantum repeaters [3]. Path entanglement is generated when a single photon is delocalized over several modes, or paths, e.g., via a 50/50 beam splitter (BS), where it produces a state of the form

$$|\Psi\rangle = \frac{1}{\sqrt{2}}(|0\rangle_A|1\rangle_B + |1\rangle_A|0\rangle_B), \tag{1}$$

where A and B denote the two entangled output modes. The versatility of this type of entanglement has been demonstrated in experiments for teleportation [4,5], entanglement swapping [6,7], purification [8], and the characterization of multipartite entanglement [9,10], and is the underlying resource for heralded photon amplification [11–13].

Another direction of interest is to use single-photon entanglement for demonstrations of quantum nonlocality and related device-independent (DI) applications. Building on initial theoretical proposals [14,15] and proof-of-principle experiments [16,17], its combination with weak displacement-based local measurements has been shown to provide a practical platform for demonstrating loophole-free Bell-inequality violations [18,19] and more efficient DI protocols for quantum information processing [20]. Notably, this approach for single-photon path entanglement offers a promising alternative to standard setups based on two-photon entanglement, with clear practical advantages, as the entanglement is heralded, and at high rates, e.g., compared to atomic systems [21–24], as well as being easily scalable to networks involving more parties [25].

Here we report the observation of Einstein-Podolsky-Rosen steering via local weak displacements performed on single-photon entanglement, as illustrated in Fig. 1. Proposed by Schrödinger, steering was only recently cast in an operational form within quantum information theory [26]. In a steering experiment, as in Fig. 1, two separate parties (Alice and Bob) share an entangled state. By performing a local measurement on her system, Alice can remotely steer the state of Bob's system. By observing this effect, Bob can verify that the shared state is indeed entangled without trusting (or equivalently, without any knowledge of) the measurements performed by Alice. This can be seen as a more stringent test of entanglement than experiments using an entanglement witness, where the measurements of both parties must be well characterized, and less stringent than a Bell inequality test, where none of the parties need to be characterized. Steering represents the key resource for one-sided DI protocols [27,28] and has recently been demonstrated in detection loophole-free

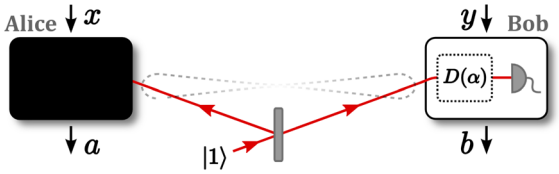

FIG. 1. Conceptual view of our steering experiment. Single-photon path entanglement is created by splitting a single photon on a beam splitter. Entanglement between the output modes of the beam splitter is certified in a one-sided DI scenario, via violation of a steering inequality. Alice's device is untrusted (black box), while Bob's device implements characterized (hence trusted) displacement-based detections where the displacement $D(\alpha)$ is a function of a measurement input y.

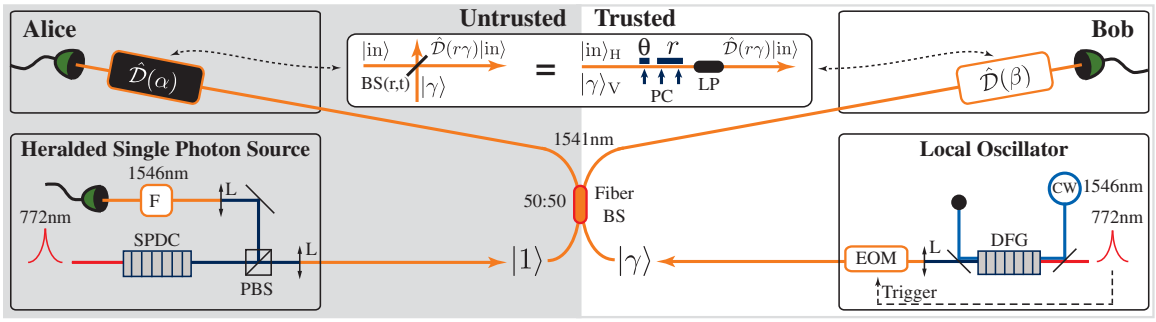

FIG. 2. Experimental setup. A heralding single-photon source is coupled into fiber and incident on a fiber BS, generating heralded entanglement, while local oscillator states, switched by an EOM, are coupled into the same BS with orthogonal polarization. Weak displacements, $\hat{\mathcal{D}}(\alpha)$, $\hat{\mathcal{D}}(\beta)$, are performed in an all-fiber configuration (inset) followed by single-photon detectors that constitute the displacement-based detection. See the main text for details and notation.

experiments in polarization [29–31] as well as single-photon entanglement, although using homodyne detection [32].

In the following, we first theoretically develop a steering test (a so-called steering inequality [33]) tailored to our scheme. We then present an experimental violation of our steering inequality by four standard deviations, using a heralded single-photon source (HSPS) and an all-fiber displacement-based measurement scheme featuring high-efficiency superconducting nanowire single-photon detectors. As our scheme is inherently free of any postselection, it is immune to the detection loophole [34]. Our experiment thus provides a conclusive demonstration of single-photon path entanglement in a one-sided DI scenario. Moreover, unlike homodyne-based schemes [32], our approach is directly extensible to a loophole-free Bell-inequality test, and thus to the implementation of fully DI protocols [21,35].

Steering.—In a steering test, as in Fig. 1., Alice remotely steers the state of Bob's system by performing a local measurement on a shared quantum state ρ. Specifically, let $\sigma_{a|x} = \mathrm{tr}[\rho(M_{a|x} \otimes \mathbb{1})]$ denote the (unnormalized) state of Bob when Alice measures x and obtains outcome a, corresponding to a measurement operator $M_{a|x}$. The set of conditional states $\{\sigma_{a|x}\}_{a,x}$ (an assemblage) is termed unsteerable if it can be created by a local strategy without using entanglement, that is, if there exists a local hidden state (LHS) model [26] compatible with it,

$$\sigma_{a|x} = \sum_{\lambda} \pi(\lambda) p(a|x\lambda) \sigma_{\lambda} \quad \forall\ a, x, \tag{2}$$

where σ_λ represents the LHS, distributed with density $\pi(\lambda)$, and $p(a|x\lambda)$ is Alice's response function. To verify steering, Bob must rule out the existence of a LHS model reproducing the data. This can be certified via violation of so-called steering inequalities [33] (analogous to Bell inequalities).

Steering inequality for displacements.—The demonstration of steering requires the use of several incompatible local measurement bases. In the case of single-photon entanglement, it is natural to consider the Fock basis, i.e., the Z basis, where perfect anticorrelations are expected for state (1). In order to access other (incompatible) bases, the use of an additional physical system must be considered, the role of which is essentially to provide a common reference frame [2,19]. Here, we consider displacement-based measurements, which consist in an optical displacement $D(\alpha)$ followed by single-photon detections (without photon-number resolution). In practice they can be implemented by interfering the mode to be measured with a weak local oscillator (LO) on a highly transmissive beam splitter, and then detecting the transmitted mode, while the reflected mode is discarded [36] (see the inset of Fig. 2). A no-click outcome corresponds to the projector $\Pi(\alpha) = |\alpha\rangle\langle\alpha|$, where $|\alpha\rangle$ is a coherent state corresponding to the displacement $\alpha = re^{i\theta}$, where $r \geq 0$ and $\theta \in [0, 2\pi]$ [14,18]. Assigning outcomes ± 1 to the click and no-click events, respectively, a displacement measurement then corresponds to the observable $M(\alpha) = 2|\alpha\rangle\langle\alpha| - \mathbb{1}$. Note that such measurements are always conclusive, as no-click events are not discarded.

Deriving a steering inequality for our setup is nontrivial because Bob's measurement operator, with binary outcomes, lives in an infinite-dimensional Hilbert space. However, we can take advantage of the fact that our target state [of the form (1)] lives in the 0–1 photon subspace, i.e., a simple qubit subspace. We thus first derive a steering inequality valid in the qubit subspace (using existing methods developed for discrete systems [37,38]) and then extend it to the full space.

Specifically, we derive a steering inequality for a scenario with four measurements for Alice ($x = 1, 2, 3, 4$) and binary output $a = \pm 1$ of the form

$$S' = \mathrm{tr}a\left[G'_R \sigma'_R + \sum_{x=1}^{4} G'_x \sigma'_{+|x}\right] \leq S'_{\max}, \tag{3}$$

where $\sigma'_R = \sigma'_{+|x} + \sigma'_{-|x}$ is the reduced state of Bob, and G'_R and G'_x are 2×2 matrices (see [39] for details). The inequality holds for any unsteerable assemblage [i.e., admitting a decomposition of the form (2)]; hence, violation of the inequality certifies steering. The bound $S'_{\max}$ is given by the largest eigenvalue of the matrices

$G'_R + \sum_x l_x G'_x$, considering any possible deterministic strategy labeled by $l_x = 0, 1$ (see [39]).

Next, we consider the restriction of $\Pi(\alpha)$ to the qubit subspace,

$$\Pi'(\alpha) = \begin{pmatrix} e^{-r^2} & e^{-r^2-i\theta}r \\ e^{-r^2+i\theta}r & e^{-r^2}r^2 \end{pmatrix}. \quad (4)$$

By choosing a set of amplitudes α_y, we can get a set of operators that spans the 2×2 space together with the identity. The G' matrices can then be resolved on these [note that the decomposition is not necessarily unique when the operators $\Pi'(\alpha_y)$ are not linearly independent],

$$G'_\nu = \sum_{y=1}^{4} c_{\nu y}\Pi'(\alpha_y) + c_{\nu 0}\mathbb{1}, \quad (5)$$

for some real coefficients $c_{\nu y}$. For our experiment, we take four settings on Bob's side (labeled by $y = 1, \ldots, 4$), given by amplitudes α_y, with fixed $r > 0$ and phases $\theta \in \{0, \pi/2, \pi, 3\pi/2\}$. The measurement outcome is denoted $b = \pm 1$. We now construct an expression analogous to (3) in the full space as follows. We define

$$S = \mathrm{tr}\left[G_R\sigma_R + \sum_{x=1}^{4} G_x\sigma_{+|x}\right], \quad (6)$$

with

$$G_\nu = \sum_{y=1}^{4} c_{\nu y}\Pi(\alpha_y) + c_{\nu 0}\mathbb{1}, \quad (7)$$

where we are no longer restricted to the 0–1 photon subspace. Similarly to S', the quantity S defines a steering inequality with the bound given by the maximal eigenvalue of the matrices $G_R + \sum_x l_x G_x$ (where as before $l_x = 0, 1$). This value can be found approximately by introducing a cutoff in photon number. We increase the cutoff until the numerically found maximal eigenvalue no longer changes. For small r, the cutoff does not need to be very large, e.g., for $r = 0.2$, a cutoff at $n \leq 4$ is sufficient. Thus, we arrive at a steering inequality $S \leq S_{\max}$. In general, the bound is larger than in the subspace, i.e., $S_{\max} > S'_{\max}$.

The expression S can be computed directly from the experimental data. Using (7) and the definitions of σ_R and $\sigma_{+|x}$ we can rewrite S in terms of the observed conditional probabilities $p(a, b|x, y)$, and obtain the steering inequality

$$S = \sum_{x,y=1}^{4} \sum_{a,b=\pm 1} c_{xy}^{ab} p(a, b|x, y) + c_0 \leq S_{\max}, \quad (8)$$

for a new set of real coefficients c_{xy}^{ab}, c_0 (see [39]). Numerical optimization shows that the violation of the above steering inequality is possible using a single-photon entangled state (1), provided the total transmission and detection efficiency is above ~43%.

Experiment.—The experimental setup is shown in Fig. 2. The HSPS is based on type-II spontaneous parametric down conversion in a PPKTP crystal satisfying the phase-matching condition 772 nm → 1541 nm + 1546 nm. The HSPS is pumped by a Ti:sapphire laser in the picosecond regime to generate pure (> 90%) photons without frequency filters [40]. The probability of generating a photon pair was set to 10^{-3}. The photons are then separated by a polarizing beam splitter. Detection of one photon at 1546 nm heralds the presence of a single photon at 1541 nm in the mode of an optical fiber with a heralding efficiency close to 80%. A 0.5 nm interference filter is placed on the heralding photon path of the HSPS so that the purity of the heralded photon approaches unity. The heralded single photon is subsequently sent to a 50:50 BS, and delocalized over two distinct spatial modes, thus producing the path entangled state (1).

To generate the LO in the same time and frequency mode as the heralded photons a second nonlinear crystal configured for difference frequency generation (DFG) is employed. For that, the crystal is pumped by the same laser as the HSPS and seeded with a cw laser at 1546 nm [41]. A delay line on the pump laser, between the two sources, is used to temporally synchronize them and is also varied to measure the Hong–Ou–Mandel (HOM) type interference, confirming the indistinguishability between the single photon and the coherent state (> 97%; see [39]). The LO is coupled into a single mode optical fiber, with an orthogonal polarization with respect to that of the path-entangled state at the same 50:50 BS used to generate the entangled state. In this way, any phase fluctuations that affect the single photon equally affect the LO, and the relative phases between the two are maintained even when propagating through fiber. At this stage the coherent states contain roughly 100 photons per pulse.

Weak displacement measurements are performed in an all-fiber configuration by Alice, $\hat{\mathcal{D}}(\alpha)$, and Bob, $\hat{\mathcal{D}}(\beta)$, interfering their respective share of the entangled state with the LO into a single polarization mode. In the inset of Fig. 2 we see the conceptual version of a displacement operation using a variable BS and the equivalent fiber implementation. This is achieved through a set of polarization rotators (PC) followed by a polarizer (LP), which effectively acts as a variable ratio BS. The polarization rotators consist of three piezo actuators that introduce small pressure-induced birefringence in the optical fiber. The polarizers project part of the LO and the photon onto the same polarization mode, where we can vary both the phase θ and amplitude r of the displacement operations.

The challenge of this experiment is to optimize each element for maximum transmission. The fields in the output modes are finally detected using MoSi superconducting nanowire single-photon detectors (SNSPD) [42]: efficiency 85%, noise 10 kHz, jitter 100 ps, and temperature 1 K. Considering the coupling efficiency of 80% and

the total transmission of all optical elements in the setup of 78% (five fiber connectors 90%, BS 98%, PC 98%, and LP 90%), we obtain a probability of 52% to detect the heralded photon in the case of no displacement. After a detection the SNSPDs are inactive for a short 100 ns recovery time, so we placed a pulse picker, based on electro-optic (amplitude) modulation (EOM), at the output of the DFG source to reduce the rate of the experiment to 9.5 MHz. We then use a logic gate to only herald entangled states when the coherent state is present, achieving a repetition rate for heralded entanglement of ~2 kHz. To perform the data analysis all the detection events are recorded using a time-to-digital converter (ID Quantique, ID801).

The bound $S_{\max}$ corresponds to an ideal displacement and perfect single-photon detection. In the experiment, the displacement is implemented using a BS of finite transmittivity, and the single-photon detectors have finite efficiency. Since Bob is a trusted party, this can, in principle, be accounted for if these parameters are measured, and leads to a lower value of the bound. However, we use the more stringent bound, which is not influenced by experimental uncertainties on the detector efficiency, i.e., that all the losses due to the detector inefficiency are considered as losses before the displacement.

To set the displacement amplitudes, we measure the probability of obtaining a detection when only the coherent state is present and obtain $r_A = 0.233 \pm 0.013$ and $r_B = 0.217 \pm 0.005$, which according to theoretical modeling should give a clear violation of (8). In order to implement the different measurement settings, we must vary the phase of the displacements. We implement an active phase change on Alice's side, while Bob's remains fixed. We vary Alice's phase (thus changing the relative phase between Alice and Bob) in small steps and record the number of detection and nondetection events. From the results, we extract the joint probabilities $p(a, b)$ as a function of Alice's phase, shown in Fig. 3.

To obtain the probabilities $p(a, b|x, y)$, we then pick four points on the curve (indicated by arrows) corresponding to $x = 1, 2, 3, 4$ and $y = 1$. In order to obtain the probabilities for $y = 2,\ 3,\ 4$, we observe that fixing Bob's phase corresponds to choosing a given reference frame. Note that the phase of the LO is not well defined; in other words there is no preferred reference frame. If the amplitude r_A is independent of the phase, then going from one frame to another (i.e., changing Bob's phase) corresponds to a permutation of the labels of Alice's measurements. Here we assume the latter, which allows us to extract all probabilities $p(a, b|x, y)$ from the data, and hence test the steering inequality.

This analysis leads to $\Delta S_{\text{exp}} = S - S_{\max} = (4.95 \pm 1.24) \times 10^{-3}$, i.e., a violation of the steering inequality by four standard deviations (error calculation details are given in Supplemental Material [39]). To cross-check this result, we fit the data of Fig. 3 to a cosine (as expected from theoretical modeling) and extract $p(a, b|x, y)$ from the fit. We obtain $\Delta S_{\text{fit}} = (2.19 \pm 1.05) \times 10^{-3}$. This is in good agreement with theoretical predictions (obtained from the estimated density matrix and experimental parameters): $\Delta S_{\text{theo}} = (3.23 \pm 0.21) \times 10^{-3}$. The fact that ΔS_{exp} gives a larger value is primarily due to the data point corresponding to maximal correlations being slightly above the fit.

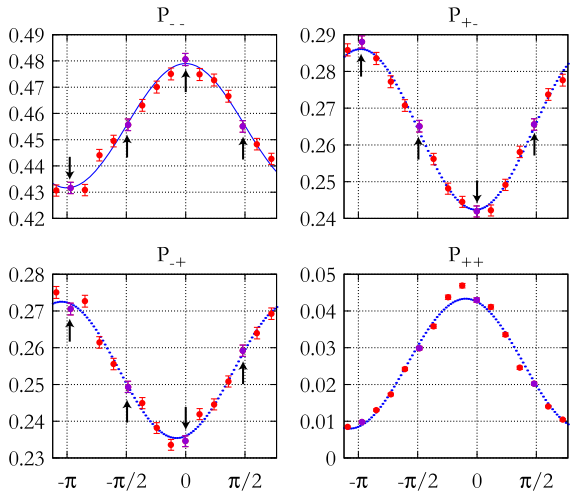

FIG. 3. Observed joint probabilities $p(a, b)$ for click and no-click events of Alice and Bob as functions of the relative phase between displacements (red points). A fit (blue lines) is used to identify which points (arrows) are used to compute the steering value. Error bars (sometimes smaller than the points) correspond to one standard deviation.

Discussion.—We have demonstrated steering of a single-photon entangled state via local weak-displacement measurements based on a novel steering inequality adapted to our setup. The four standard deviation violation represents a conclusive measurement of single-photon entanglement in a one-sided DI scenario, with applications to partially DI protocols, such as one-sided DI cryptography.

As our setup is completely free of any postselection, it is, in principle, directly amenable to a loophole-free Bell inequality test. This requires increasing the global detection efficiency from about 50% to more than 83.5% for a bipartite test, or > 74% for four-partite Bell tests with three settings per party. As efficiencies of 75% have already been achieved in the bipartite case [43,44], and three-partite single-photon entanglement has been demonstrated [25], the prospects are promising. In particular, the losses due to optical elements can be significantly reduced by removing the fiber connectors, currently used for alignment, e.g., by splicing, as well as incorporating approaches of Refs. [43,44] to implement the polarization projection for the displacements. This platform thus has clear potential for future implementations of DI and semi-DI protocols at high rates.

The authors thank Natalia Bruno for assistance with the HSPS and LO setups. This work was supported by the Swiss national science foundation (Grant

No. 200021_159592 and starting grant DIAQ), the NCCR-QSIT, the OTKA Grant No. K111734, as well as the EU project SIQS Grant No. 600645. NIST acknowledges funding from the DARPA QUINESS program. Part of the research on the detectors was carried out at the Jet Propulsion Laboratory, California Institute of Technology, under a contract with the National Aeronautics and Space Administration.

*nicolas.brunner@unige.ch
†robert.thew@unige.ch

[1] S. M. Tan, D. F. Walls, and M. J. Collett, Phys. Rev. Lett. **66**, 252 (1991).
[2] S. J. van Enk, Phys. Rev. A **72**, 064306 (2005).
[3] N. Sangouard, C. Simon, H. de Riedmatten, and N. Gisin, Rev. Mod. Phys. **83**, 33 (2011).
[4] E. Lombardi, F. Sciarrino, S. Popescu, and F. De Martini, Phys. Rev. Lett. **88**, 070402 (2002).
[5] M. Fuwa, S. Toba, S. Takeda, P. Marek, L. Mišta, R. Filip, P. van Loock, J.-I. Yoshikawa, and A. Furusawa, Phys. Rev. Lett. **113**, 223602 (2014).
[6] F. Sciarrino, E. Lombardi, G. Milani, and F. De Martini, Phys. Rev. A **66**, 024309 (2002).
[7] C. I. Osorio, N. Bruno, N. Sangouard, H. Zbinden, N. Gisin, and R. T. Thew, Phys. Rev. A **86**, 023815 (2012).
[8] D. Salart, O. Landry, N. Sangouard, N. Gisin, H. Herrmann, B. Sanguinetti, C. Simon, W. Sohler, R. T. Thew, A. Thomas, and H. Zbinden, Phys. Rev. Lett. **104**, 180504 (2010).
[9] S. B. Papp, K. S. Choi, H. Deng, P. Lougovski, S. J. van Enk, and H. J. Kimble, Science **324**, 764 (2009).
[10] M. Gräfe, R. Heilmann, A. Perez-Leija, R. Keil, F. Dreisow, M. Heinrich, H. Moya-Cessa, S. Nolte, D. N. Christodoulides, and A. Szameit, Nat. Photonics **8**, 791 (2014).
[11] T. C. Ralph and A. P. Lund, AIP Conf. Proc. **1110**, 155 (2009).
[12] S. Kocsis, G. Y. Xiang, T. C. Ralph, and G. J. Pryde, Nat. Phys. **9**, 23 (2013).
[13] N. Bruno, V. Pini, A. Martin, V. B. Verma, S. W. Nam, R. Mirin, A. Lita, F. Marsili, B. Korzh, F. Bussières, N. Sangouard, H. Zbinden, N. Gisin, and R. T. Thew, Opt. Express **24**, 125 (2016).
[14] K. Banaszek and K. Wódkiewicz, Phys. Rev. Lett. **82**, 2009 (1999).
[15] G. Björk, P. Jonsson, and L. L. Sánchez Soto, Phys. Rev. A **64**, 042106 (2001).
[16] A. Kuzmich, I. A. Walmsley, and L. Mandel, Phys. Rev. Lett. **85**, 1349 (2000).
[17] B. Hessmo, P. Usachev, H. Heydari, and G. Björk, Phys. Rev. Lett. **92**, 180401 (2004).
[18] J. B. Brask and R. Chaves, Phys. Rev. A **86**, 010103 (2012).
[19] J. B. Brask, R. Chaves, and N. Brunner, Phys. Rev. A **88**, 012111 (2013).
[20] V. C. Vivoli, P. Sekatski, J. D. Bancal, C. Lim, A. Martin, R. Thew, H. Zbinden, N. Gisin, and N. Sangouard, New J. Phys. **17**, 023023 (2015).
[21] S. Pironio, A. Acin, S. Massar, A. B. de la Giroday, D. N. Matsukevich, P. Maunz, S. Olmschenk, D. Hayes, L. Luo, T. A. Manning, and C. Monroe, Nature (London) **464**, 1021 (2010).
[22] J. Hofmann, M. Krug, N. Ortegel, L. Gerard, M. Weber, W. Rosen, and H. Weinfurter, Science **337**, 72 (2012).
[23] S. Ritter, C. Nölleke, C. Hahn, A. Reiserer, A. Neuzner, M. Uphoff, M. Mücke, E. Figueroa, J. Bochmann, and G. Rempe, Nature (London) **484**, 195 (2012).
[24] B. Hensen, H. Bernien, A. Dréau, A. Reiserer, N. Kalb, M. Blok, J. Ruitenberg, R. Vermeulen, R. Schouten, C. Abellán, W. Amaya, V. Pruneri, M. W. Mitchell, M. Markham, D. Twitchen, D. Elkouss, S. Wehner, T. Taminiau, and R. Hanson, Nature (London) **526**, 682 (2015).
[25] F. Monteiro, V. C. Vivoli, T. Guerreiro, A. Martin, J. D. Bancal, H. Zbinden, R. T. Thew, and N. Sangouard, Phys. Rev. Lett. **114**, 170504 (2015).
[26] H. M. Wiseman, S. J. Jones, and A. C. Doherty, Phys. Rev. Lett. **98**, 140402 (2007).
[27] C. Branciard, E. G. Cavalcanti, S. P. Walborn, V. Scarani, and H. M. Wiseman, Phys. Rev. A **85**, 010301 (2012).
[28] M. Tomamichel and R. Renner, Phys. Rev. Lett. **106**, 110506 (2011).
[29] B. Wittmann, S. Ramelow, F. Steinlechner, N. K. Langford, N. Brunner, H. M. Wiseman, R. Ursin, and A. Zeilinger, New J. Phys. **14**, 053030 (2012).
[30] D. H. Smith, G. Gillett, M. P. de Almeida, C. Branciard, A. Fedrizzi, T. J. Weinhold, A. Lita, B. Calkins, T. Gerrits, H. M. Wiseman, S. W. Nam, and A. G. White, Nat. Commun. **3**, 625 (2012).
[31] A. J. Bennet, D. A. Evans, D. J. Saunders, C. Branciard, E. G. Cavalcanti, H. M. Wiseman, and G. J. Pryde, Phys. Rev. X **2**, 031003 (2012).
[32] M. Fuwa, S. Takeda, M. Zwierz, H. M. Wiseman, and A. Furusawa, Nat. Commun. **6**, 6665 (2015).
[33] E. G. Cavalcanti, S. J. Jones, H. M. Wiseman, and M. D. Reid, Phys. Rev. A **80**, 032112 (2009).
[34] N. Brunner, D. Cavalcanti, S. Pironio, V. Scarani, and S. Wehner, Rev. Mod. Phys. **86**, 419 (2014).
[35] A. Acín, N. Brunner, N. Gisin, S. Massar, S. Pironio, and V. Scarani, Phys. Rev. Lett. **98**, 230501 (2007).
[36] M. G. A. Paris, Phys. Lett. A **217**, 78 (1996).
[37] M. F. Pusey, Phys. Rev. A **88**, 032313 (2013).
[38] P. Skrzypczyk, M. Navascués, and D. Cavalcanti, Phys. Rev. Lett. **112**, 180404 (2014).
[39] See Supplemental Material http://link.aps.org/supplemental/10.1103/PhysRevLett.117.070404 for details about the numerical procedure to obtain the steering inequality and its extension to the full Fock space, the procedure to calculate the error bars on the violation, measurements performed to temporally align the single photons and coherent state, and determining the indistinguishability between them.
[40] N. Bruno, A. Martin, T. Guerreiro, B. Sanguinetti, and R. T. Thew, Opt. Express **22**, 17246 (2014).
[41] N. Bruno, A. Martin, and R. Thew, Opt. Commun. **327**, 17 (2014).
[42] V. B. Verma, B. Korzh, F. Bussières, R. D. Horansky, S. D. Dyer, A. E. Lita, I. Vayshenker, F. Marsili, M. D. Shaw, H. Zbinden, R. P. Mirin, and S. W. Nam, Opt. Express **23**, 33792 (2015).
[43] L. K. Shalm *et al.*, Phys. Rev. Lett. **115**, 250402 (2015).
[44] M. Giustina *et al.*, Phys. Rev. Lett. **115**, 250401 (2015).